ELSEVIER

Thermochimica Acta 260 (1995) 165–185

thermochimica acta

Bismuth and mixed bismuth–lanthanide carboxylates as precursors for pure and Ln-promoted bismuth molybdate catalysts

M. Devillers *,[1], F. De Smet, O. Tirions

Université Catholique de Louvain, Laboratoire de Chimie Inorganique et Analytique, place Louis Pasteur, 1, B-1348 Louvain-la-Neuve, Belgium

Received 25 August 1994; accepted 20 January 1995

Abstract

Several bismuth(III) carboxylates (formate, acetate, propionate, oxalate, lactate) and the analogous tervalent lanthanum, samarium and praseodymium formates and acetates were synthesized and characterized in view of their use as precursors for the formation of bismuth- or lanthanide-based molybdate catalysts upon controlled thermal decomposition on MoO_3 support. Mixed Bi–Ln carboxylates were prepared and used in parallel as precursors for Ln-promoted bismuth molybdate catalysts. Both the nature of the lanthanide element and the calcination temperature were found to determine the formation of specific molybdate-type phases on the support. Detailed examination of these catalysts by X-ray diffraction and FTIR spectroscopy identified α-$M_2Mo_3O_{12}$ phases in Bi- and Pr-containing samples calcined at 823 K, and hexamolybdate phases $M_2Mo_6O_{21}$ in La- or Sm-containing catalysts calcined at 973 K.

Keywords: Acetates; Bismuth; Formates; Lanthanides; Molybdates

1. Introduction

Precursor methods continue to attract considerable interest as an original approach to generate homogeneously dispersed solid state materials such as oxides [1–3], sulphides [4, 5], carbides and nitrides [6], which are key compounds not only for the development of new superconductors and composite ceramics [7], but also in thin film

* Corresponding author.

[1] Research Associate of the Belgian National Fund for Scientific Research.

SSDI 0040-6031(95)02286-4

technology and in the broad area of heterogeneous catalysts. In a recent IUPAC monograph published in the series "Chemistry for the 21st Century", an updated review of the state of the art in the preparation of so-called "advanced materials" surveyed the current strategies [8].

As far as oxides are concerned, controlled pyrolysis of amorphous citrate or oxalate-type precursors has long been known as an appropriate way to synthesize highly dispersed mixed oxides and oxide solid solutions [9, 10]. Numerours applications can be found in the literature in the respective fields of high-T_c superconductors [11–14] and perovskites [15–17]. As regards oxide-type heterogeneous catalysts, the use of carboxylates offers several advantages: (i) these compounds exhibit usually well-defined structures and stoichiometries depending on the nature of the carboxylate chain; (ii) they can be designed to contain no heteroelement apart from carbon, nitrogen, oxygen and hydrogen, thus preventing eventual poisoning or alteration of the catalyst by elements like sulphur or halogens; (iii) their multidentate structure often favours the formation of polymeric patterns which can help to control the distribution of the active metals on the surface; and (iv) the thermal decomposition of these ligands into well-defined and finely dispersed powdered samples occurs at moderate temperatures that allow sintering effects to be limited.

Mixed systems which are heterometallic in nature are of great interest in controlling the polymetallic activation process in catalysis. The properties of these systems are related to the respective behaviour of the involved cations: among the different relevant parameters, geometric and steric factors like the ionic radius and the coordination number are particularly important. With respect to this, the association of bismuth and lanthanides is perfectly adequate: in a given coordination geometry, La^{3+} and Bi^{3+} cations actually display identical ionic radii [18] and, considering the lanthanide contraction effect, substitutional replacement of bismuth atoms by lanthanum or other lanthanides should be a favoured process.

The present work was undertaken in the framework of a research programme dealing with the control of the structure of bismuth-based multimetallic oxide catalysts. Bismuth is indeed currently used as a promoting element in heterogeneous catalysis, particularly in the field of selective oxidations; the most well-known system is the family of bismuth molybdate catalysts which are involved in acrolein synthesis from propene and in the propene ammoxidation process leading to acrylonitrile. Most industrial catalysts based on the Bi–Mo system contain, however, additional elements such as phosphorus, vanadium, or many others, which are responsible for significant changes in overall catalytic activity and/or selectivity [19]. This work deals more specifically with the partial replacement of bismuth by rare earth elements, which are indeed known to play an active role in oxidative environmental catalysis. Among different applications, lanthanide-based perovskites are useful as catalysts for the conversion of CO into CO_2 [20], NO into N_2 [20], and for the total oxidation of hydrocarbons [21]; pure lanthanide oxides are able to catalyse NO conversion into NO_2 [22] and are efficient for the oxidative coupling of methane [23]. Although the catalytic potential of these elements seems to be mainly focussed on the total oxidation processes, experimental results that suggest they could play an essential role in controlling selective oxidation have been reported in the literature. These data all concern the implementa-

tion of Mo–Pr–O or Mo–Bi–Pr–O systems for the propene/acrolein or isobutene/methacrolein oxidation reactions [24–28]. The exact role played by these elements in the general area of oxidation catalysis remains, however, unclear; this justifies an examination of the modification of Bi–Mo catalysts by incorporation of lanthanide elements.

The present paper mainly describes the preparation and characterization of lanthanide-modified bismuth molybdate catalysts in which bismuth has been replaced by lanthanum, samarium or praseodymium. The literature reports on the incorporation of rare earth elements in perovskite-type compounds by using cyanide [29, 30], oxalate [29, 31] or citrate [29, 32, 33] complexes as starting materials. In this work, short-chain linear carboxylates of these elements, in pure or mixed form, were selected as solid state precursors. The synthesis, solid-state characterization and thermal degradation properties of these precursors will be reviewed. The nature of the final molybdate catalysts obtained after reaction with MoO_3 will be examined through X-ray diffraction and infra-red spectroscopy. As well the nature of the lanthanide, the bismuth-to-lanthanide ratio and the overall (Bi + Ln)-to-Mo ratio in these phases were considered as interesting variables.

2. Experimental

2.1. Chemical syntheses of bismuth and lanthanide precursors

2.1.1. Formates

Bismuth(III) triformate, $Bi(HCO_2)_3$ (denoted hereafter as $BiFm_3$) was prepared according to the literature [34] by refluxing bismuth(III) oxide in water in the presence of an excess of formic acid. The crystals were washed with acetone and dried in ambient air without showing any degradation. The corresponding pure lanthanide $LnFm_3$ and mixed bismuth–lanthanide compounds $(Ln, Bi)Fm_3$ (Bi/Ln = 0.33, 1.0 or 3.0) were obtained similarly for Ln being La, Sm or Pr, starting from La_2O_3, Sm_2O_3 or Pr_6O_{11} in appropriate amounts.

2.1.2. Acetates

Bismuth(III) triacetate, $Bi(CH_3CO_2)_3$ (denoted hereafter as $BiAc_3$) was obtained according to the literature by refluxing bismuth(III) oxide in a 1:1 (vol:vol) mixture of acetic acid and acetic anhydride [35]. After cooling down to 273 K, white crystals were separated from the parent solution, then dried and stored under nitrogen to prevent hydrolysis to bismuth oxoacetate. Lanthanum(III) acetate and a mixed (Bi, La) acetate with Bi/La = 1.0 were prepared according to the same procedure from La_2O_3.

2.1.3. Bismuth(III) tripropionate

Bismuth(III) tripropionate, $Bi(C_2H_5CO_2)_3$ (denoted hereafter as $Bi(prop)_3$) was synthesized by refluxing Bi_2O_3 in a 1:1 (vol:vol) mixture of propionic acid and propionic anhydride. White crystals were collected after cooling down to 273 K, dried by vacuum heating at 313 K, and finally stored under nitrogen atmosphere.

2.1.4. Bismuth(III) oxalate

Anhydrous bismuth(III) oxalate, $Bi_2(C_2O_4)_3$ (denoted hereafter as Bi_2Ox_3) was obtained by thermal decomposition of the heptahydrate at 473 K for 3 h. $Bi_2(C_2O_4)_3 \cdot 7H_2O$ was precipitated in water at 330 K from $Bi(NO_3)_3 \cdot 5H_2O$ and an excess of oxalic acid in the presence of mannitol, according to a literature procedure [36].

2.1.5. Bismuth(III) dilactate

Anhydrous bismuth(III) dilactate, $BiC_6H_9O_6$, (denoted hereafter as $Bi(lact)_2$) was obtained by dehydration of the heptahydrated compound, $BiC_6H_9O_6 \cdot 7H_2O$, at 498 K for 2 h. The hydrated precursor was prepared by refluxing Bi_2O_3 in a slight excess of d-l lactic acid for 4.5 h. After concentrating the solution at 373 K, a white product separated as the solution was cooled down; after filtration, the precipitate was washed with acetone and ether, then dried in air for a few minutes.

2.2. Preparation of the MoO_3-supported molybdate catalysts

2.2.1. Molybdenum(VI) oxide

MoO_3, exhibiting a specific surface area of $2.0 \pm 0.2\ m^2\ g^{-1}$, was obtained by calcination of a citrate-type complex at 673 K for 20 h. The citrate precursor was synthesized from solutions of ammonium heptamolybdate ($0.2\ mol\ l^{-1}$) and citric acid ($1.6\ mol\ l^{-1}$); the gel obtained after partial elimination of water was subsequently heated under vacuum at 363 K for 20 h, and then, after grinding, at 573 K in air for a further 20 h.

2.2.2. Molybdate catalysts

Molybdate catalysts were prepared from carboxylate precursors according to a deposition procedure carried out in dry *n*-heptane under nitrogen. The molar ratio (Ln + Bi)/Mo was taken at 0.125, by referring to catalytic results described in the literature [24] showing that selectivity of Mo–Pr–O catalysts for acrolein formation from propene reached a maximum value at Mo/(Mo + Pr) = 0.8–0.88. The adequate amount of carboxylates was initially dispersed under ultrasonic stirring in 100 ml distilled *n*-heptane; 15 min later, the molybdenum oxide support (2 g) was added to the flask and the system was submitted to further sonication for another 15 min period. The organic solvent was then slowly eliminated up to dryness, and the solid obtained was calcined overnight in air at 823 K (monometallic Bi- or Pr-based catalysts) or 973 K (La- or Sm-based catalysts). These temperatures were selected as a consequence of the thermal behaviour of the various precursors, as described below in Section 3.

Some comparative catalysts were prepared by an impregnation method starting from lanthanide nitrates in aqueous solution at pH 2. Water was first eliminated in a rotatory evaporator at 338 K, then in a dry oven at 383 K for 1 h; the catalysts were finally calcined overnight in air at 823 K.

2.3. Chemical analysis

The bismuth or lanthanide content was determined by complexometric titration with EDTA in the presence of xylenol orange. As indicated by the respective formation

constants of the concerned EDTA complexes, the method can readily be applied to mixed Bi–Ln compounds: Bi is titrated first at pH values of between 0 and 1; then the lanthanide element, after pH adjustment to 6 with hexamethylenetetramine.

2.4. Instrumental analysis

Infrared spectra were registered in the form of KBr pellets on a Perkin-Elmer type 1710 Fourier transform spectrometer operating in the range 4000–450 cm^{-1}.

Thermogravimetric analysis was performed in air with a Setaram TGC 85 analyser at a heating rate of 20 K min^{-1}. The reported transition temperatures were calculated from the differential DTG curve.

Powder X-ray diffraction spectra were measured on a Siemens 500 diffractometer equipped with a copper anode.

The BET specific surface areas of the MoO_3 support and of some of the Bi_2O_3 powders obtained in this work were measured with a Micromeritics ASAP 2000 analyser, using krypton gas at 77 K.

3. Results and discussion

3.1. Characterization of monometallic precursors

With the exception of praseodymium triformate which, as far as we know, has never been mentioned in the literature, all the reported compounds selected here as precursors of molybdate-type catalysts have been described previously, at least partially, from the point of view of either their IR characterization or thermal decomposition properties. Considering the fact that the concerned data are sometimes more than twenty years old, it is of some interest to report briefly the main characteristics relevant to the present work.

3.1.1. Bismuth(III) formate, $Bi(HCO_2)_3$

According to the literature, bismuth triformate has a trigonal structure characterized by a polymeric layer arrangement in which Bi atoms are coordinated by nine oxygen atoms at various distances: 238, 252 and 277 pm [34]. The IR spectrum of the synthesized compound (% Bi: exp., 60.7; theor., 61.1) exhibits absorption bands at 1550 (s, br; ν_{as}(COO)), 1387 (s, sh; δ(COO) or δ(CH)), 1325 (s, br; ν_s(COO)), 788 and 772 (m; δ_s(COO)) cm^{-1}, in good agreement with literature values [35, 37]. When exposed to ambient air, partial hydrolysis is detected by the appearance of a low, intense, broad band at 570 cm^{-1} which is characteristic of $BiO(HCO_2)$ [38]. As already mentioned [39], the $\Delta\nu$ value between the symmetric and asymmetric stretching modes of the carboxylate group (225 cm^{-1}), which is in some way related to the coordination mode of the ligand around the metal, is very similar to the value observed in alkali metal formates (230 cm^{-1}); the presence of additional Bi–O interactions in the crystal structure is, however, responsible for a 40 cm^{-1} shift of these two absorption bands.

The TGA curve in air shows only one decomposition step at 483 K into Bi_2O_3.

3.1.2. Bismuth(III) triacetate, $Bi(CH_3CO_2)_3$

Depending on the crystallinity of the obtained compound, powder samples of Bi(III) acetate are shown to be extremely sensitive towards hydrolysis in ambient air, causing significant conversion into Bi(III) oxoacetate, $BiO(CH_3CO_2)$, with liberation of acetic acid. This hydrolysis process can be easily followed by IR spectroscopy on air-exposed powder samples, by the growth of an IR band at about 530 cm^{-1}, characteristic of the Bi–O bond in bismuthyl salts [40]. Samples prepared from the mixed acetic acid/anhydride procedure and precipitated by cooling down to 273 K were found to contain larger crystals which are definitely more resistant to degradation. The infrared data are in good agreement with previously published values [35, 37, 41]. The wavenumber difference between the two bands arising from the symmetric and antisymmetric stretching modes (1397 and 1544 cm^{-1}), i.e. 147 cm^{-1}, is *a priori* compatible with either a bridged structure, or with a chelate-type structure [39]. It should be noted that this value is virtually identical with that observed in dihydrated cadmium acetate (146 cm^{-1} [42]), in which both types of metal coordination appear simultaneously [43], one of the oxygen atoms of the acetate group being involved in metal–oxygen bonds with two neighbouring metal atoms. This is in total agreement with the crystal structure of bismuth acetate as described recently in the literature [44]: all the acetate groups behave as bidentate ligands with Bi–O distance smaller than 265 pm; some of them are involved in additional interactions at longer range (281, 283, 294 pm) with bismuth atoms belonging to a parallel sheet. The resulting coordination sphere is a nine-vertices distorted polyhedron with fourteen triangular faces, whose dissymmetry is caused by the presence of the lone pair on the bismuth atom.

Thermal decomposition into Bi_2O_3 proceeds at 613 K through an intermediate step corresponding to bismuth oxoacetate.

3.1.3. Bismuth(III) tripropionate, $Bi(C_2H_5CO_2)_3$

The main IR absorption bands of Bi(III) tripropionate (%Bi: exp., 48.3; theor., 48.8) appear at the following wavenumber values (cm^{-1}): 2979 (m), 2942 (m), 2883 (w), 1720 (m), 1544 (vs, br), 1465 (s), 1402 (vs, br), 1367 (s, sh), 1284 (s, br), 1077 (m), 1009 (w), 895 (m), 813 (m), 630 (m, br), 496 (m, br). Upon heating in air, decomposition into Bi_2O_3 starts at 423 K and is complete at 660 K.

3.1.4. Bismuth(III) oxalate, $Bi_2(C_2O_4)_3$

Poorly resolved IR spectra are obtained with the anhydrous compound, showing bands at 2336 (w), 1565–1545 (s, br), 1385 (m), 1279 (m, br), 900 (w), 783 (m) and 476 (m, br) cm^{-1}. Detailed thermal degradation experiments on the heptahydrated compound suggest that dehydration proceeds through two steps corresponding to the release of six and one water molecule, respectively. Heating overnight at 383 K provides the monohydrate, the anhydrous compound being obtained after further heating at 423 K (total weight loss at 293–423 K: exp., 15.7%; theor. for $7H_2O$, 15.6%). Further degradation into Bi_2O_3 with CO/CO_2 evolution occurs at 538 K.

3.1.5. *Bismuth(III) dilactate, $Bi(C_6H_9O_6)$*

This compound has been mentioned briefly in old literature [45] and corresponds to the formulation $Bi(C_3H_4O_3)(C_3H_5O_3)$ in which one of the two lactate ligands is doubly ionized. The heptahydrate (%Bi: exp., 40.1; theor., 40.8) is thermally decomposed into Bi_2O_3 in three successive steps corresponding respectively to the formation of the pentahydrated compound (443 K) and the anhydrous lactate (543 K). The main IR bands of the anhydrous compound appear at the following wavenumber values (cm^{-1}): 3403 (s, br), 1602 (vs, br), 1572 (vs, br), 1470 (m), 1448 (m), 1412 (s), 1375 (vs), 1350 (vs), 1312 (s), 1294 (vs), 1132 (s), 1108 (s), 1048 (vs), 920 (m), 865 (m), 852 (s), 773 (m), 775 (m), 708 (s), 666 (m), 614 (m), 579 (s), 566 (s) and 520 (s).

3.1.6. *Lanthanum(III) triformate, $La(HCO_2)_3$*

IR and thermal decomposition data were reported previously in the literature [46, 47]. The main IR absorption bands obtained with our samples are listed in Table 1 and compared with literature values. The TGA curve obtained in air displays two well-defined decomposition steps at 693 and 1048 K, corresponding to the formation of the oxocarbonate $La_2O_2CO_3$ and the oxide La_2O_3, respectively. In line with the pronounced hygroscopic character of this oxide, the presence of lanthanum(III) hydroxide was systematically detected by X-ray diffractometry.

3.1.7. *Lanthanum(III) triacetate, $La(CH_3CO_2)_3$*

Infrared and thermal decomposition studies on lanthanum triacetate were reported previously in the literature [48, 49]. As shown in Fig. 1(a), the IR bands associated with the stretching modes of the carboxylate group are split as a consequence of the presence of multiple metal–oxygen bonding types (Ln–O and Ln–O–Ln) in a polymeric structure. Thermal decomposition into La_2O_3 occurs in four successive steps at 623, 673, 723 and 1043 K, with the following intermediate compounds: the acetatocarbonate $La(CH_3CO_2)CO_3$, the carbonate $La_2(CO_3)_3$, and the oxocarbonate $La_2O_2CO_3$.

Table 1
Infrared absorption bands of lanthanide triformates $Ln(HCO_2)_3$ (Ln is La, Sm, Pr)

$La(HCO_2)_3$			$Sm(HCO_2)_3$		$Pr(HCO_2)_3$ This work	Band assignment
This work	Ref. [46]	Ref. [47]	This work	Ref. [47]		
2913 (w)	2856				2914 (vw)	ν(CH)
2694 (vw)						
1608 (vs, br)	1605		1608 (vs, br)		1603 (vs, br)	ν_{as}(COO)
1578 (vs)	1580	1575	1578 (vs)	1575	1575 (vs)	
1428 (s)	1428				1430 (s)	δ_{as}(COO) + δ(CH)
1406 (s)	1405	1388	1409 (s)	1410	1405 (s)	
1359 (s)	1358	1356	1361 (vs)	1360	1358 (s)	ν_s(COO)
			1096 (s)	1095		π(COO) + π(CH)
780 (s)	779	773	785 (s)	777	780 (s)	δ_s(COO)

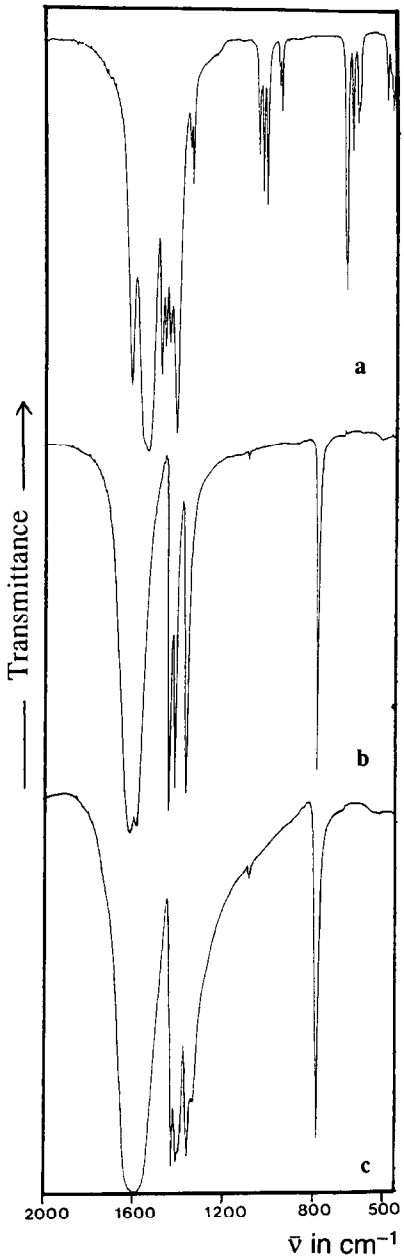

Fig. 1. Infrared spectra of (a) lanthanum(III) triacetate, (b) praseodymium(III) triformate and (c) mixed bismuth–lanthanum (1:1) triformate.

3.1.8. Samarium(III) triformate, $Sm(HCO_2)_3$

The main IR data are listed in Table 1 together with literature values [47]. Thermal degradation in air proceeds in two successive steps at 703 and 933 K, the oxocarbonate $Sm_2O_2CO_3$ appearing again as the intermediate compound.

3.1.9. Praseodymium(III) triformate, $Pr(HCO_2)_3$

As far as we know, this compound has never been described in the literature before now. The X-ray powder diffraction pattern is characterized by the following *d* values (pm) and relative intensities: 534.3 (100), 374.5 (4), 307.8 (15), 266.5 (78), 216.9 (9), 201.3 (20), 188.0 (7), 177.6 (20), 168.1 (2), 160.3 (4), 153.7 (6), 147.6 (6), 133.1 (8), 125.3 (2), 122.1 (4), 116.2 (2). The analogy with the corresponding values characteristic of other lanthanide formates is obvious, particularly with those of the neodymium compound $Nd(HCO_2)_3$. The main IR absorption bands (Fig. 1(b)) are listed in Table 1 and are very similar to those of lanthanum and samarium formates. Fig. 2 illustrates the thermal behaviour of this compound when heated in air up to 1173 K. Two successive weight losses occur at 723 and 863 K, respectively. The oxocarbonate $Pr_2O_2CO_3$ can be postulated again as the intermediate product (theor. weight loss, 32.3%); the final residue has been identified as the mixed-valence oxide Pr_6O_{11} by X-ray diffractometry.

3.2. Characterization of bimetallic precursors

3.2.1. Mixed Bi–La (1:1) formate

The formation of bimetallic mixed crystals $Bi_xLa_{1-x}(HCO_2)_3$ is suggested by the X-ray diffraction pattern of the obtained powder. The calculated interreticular spacings (*d*) are listed in Table 2 together with the corresponding parameters obtained experi-

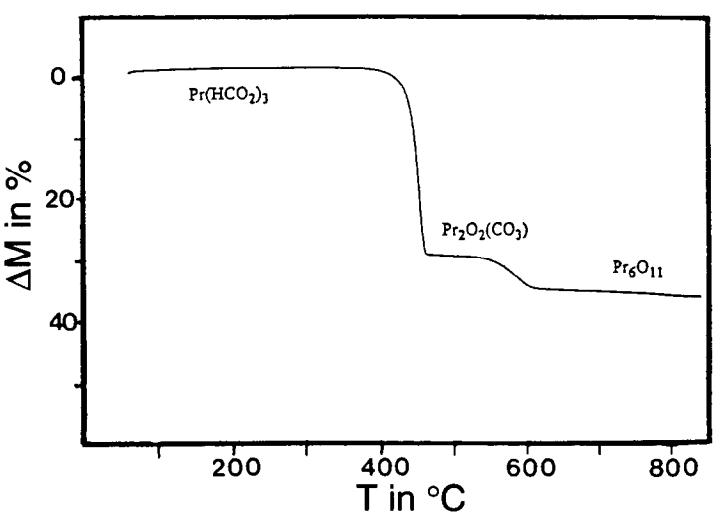

Fig. 2. Thermogravimetric analysis of praseodymium(III) triformate in air (heating rate, 20 K min^{-1}).

Table 2
Experimental values of the interreticular spacing in pure and mixed bismuth and lanthanum formates

$Bi(HCO_2)_3$		$La(HCO_2)_3$		Bi–La(1:1) formate
d/pm exp.	*d*/pm ASTM	*d*/pm exp.	*d*/pm ASTM	*d*/pm exp.
531.0	535.6	540.1	541	529.2
377.0	377.8	379.9	379	375.7
306.8	305.8	310.6	309	303.3
264.8	266.0	268.9	268	264.0
216.5	216.8	219.3	219	214.8
200.1	200.8	203.2	202	199.4
187.4	187.7	189.9	189	186.1
176.4	176.8	179.2	178	175.9
167.5	167.5	169.9	169	166.5

mentally with the pure phases. Reference *d* values taken from the ASTM database are given for comparison. Instead of superimposed diffraction patterns, a new diffractogram appears in which all the diffraction peaks are shifted towards lower *d* values with respect to the two pure phases. In the same way, modifications are observed in the IR spectrum which displays a completely different shape: the well-defined doublet appearing at 788–772 cm^{-1} in pure bismuth formate is replaced by a single band at 780 cm^{-1}, as in the pure lanthanum compound, whereas several shape and intensity changes are noted in the 1300–1600 cm^{-1} region (see Fig. 1(c)). In the TGA curve recorded in the same experimental conditions as for the pure compounds, the formation of a mixed phase is confirmed by the appearance of new decomposition stages characterized by transition temperatures of 488, 533, 623 and 1033 K. The bismuth-to-lanthanum ratio determined by chemical analysis being close to 1.00, this compound can be formulated as $Bi_{0.5}La_{0.5}(HCO_2)_3$.

3.2.2. *Mixed Bi–Sm (1:1) formate*

As in the previous case, the formation of a mixed Bi–Sm compound is suggested by the X-ray diffraction data although the variations concerned are less pronounced than in the Bi–La case. The similarity between the parameters of this mixed phase and those of pure bismuth formate suggests, nevertheless, that the latter lattice is globally preserved upon partial replacement of Bi by smaller Sm ions. The corresponding IR spectrum shows absorption bands at 1572, 1397, 1353 and 780 cm^{-1}, positions which are close to those of the reference bands in the pure compounds. The thermal behaviour of the mixed compound is characterized by two successive decomposition steps at 488 and 538 K; the weight losses reported at 703 and 933 K for the pure samarium compound are clearly absent. Complementary information on the thermal behaviour and the nature of the degradation products will be given further in this paper. The bismuth-to-metal ratio determined by chemical analysis is found to be 1.00, in line with the formulation $Bi_{0.5}Sm_{0.5}(HCO_2)_3$.

3.2.3. Mixed Bi–Pr (3:1), (1:1) and (1:3) formates

The chemical composition of these phases was checked by chemical analysis of Bi and Pr. The Bi-to-Pr molar ratios were found to be 0.32, 1.00 and 3.09, respectively, suggesting the formulations $Bi_{0.24}Pr_{0.76}(Fm)_3$, $Bi_{0.5}Pr_{0.5}(Fm)_3$ and $Bi_{0.76}Pr_{0.24}(Fm)_3$ for the mixed compounds obtained.

When comparing the XRD data of the mixed and pure compounds, most of the characteristic peaks of the pure phases also appear in the mixed compounds with relative intensities in relationship with the Bi/Pr molar ratio. Additional lines are nevertheless observed which do not correspond to these pure phases. Similar conclusions can be drawn on the basis of the infrared spectra. These data suggest the simultaneous presence of mixed $Bi_{1-x}Pr_x(Fm)_3$ phases together with a mixture of the corresponding pure compounds.

The TGA curve of the equimolar Bi–Pr compound shows three successive decomposition steps at 500, 550 and 633 K. The last two steps are found to occur at temperatures which are significantly lower than in pure Pr formate.

3.2.4. Mixed Bi–La (1:1) acetate

The equimolecular composition of this phase was checked by chemical analysis of the two metals. Both IR and TGA results are very similar to those of the individual components. In particular, the positions of the infrared bands are very close to those of pure La(III) acetate: main bands are observed at 1603 (s), 1527 (vs), 1473 (s), 1453 (s), 1440 (s, sh), 1407 (vs), (1339) (m), 1052 (w), 1033 (w), 1016 (m), 964 (w), 953 (w), 664 (m), (641 (w), 612 (w), 490 (w) and 467 (w) cm^{-1}. Thermal decomposition occurs in three successive steps at 553, 638 and 1043 K.

3.3. General comments on the mixed Bi–Ln compounds

As mentioned earlier in the sections devoted to the characterization of individual compounds, some general comments concerning the structure of the investigated mixed Bi–Ln carboxylates can be formulated by taking into account two specific experimental parameters, namely the difference between the IR wavenumber values associated with the symmetric and asymmetric stretching modes, $\Delta\nu = \nu_{as}(COO) - \nu_s(COO)$; and the evolution of the interreticular spacings d associated with a given diffraction line.

Selected results are presented in Table 3, together with the Shannon–Prewitt crystal radii of the concerned tervalent ions, in either six-fold or nine-fold coordination geometries [18].

In the formate case, the similarity of the $\Delta\nu$ values suggests the presence of analogous coordination modes. If one refers to the literature data concerning bismuth(III) formate, this structure has a polymeric nature in which the formate ligands occupy bridging positions between neighbouring metal ions and are simultaneously linked to another metal atom belonging to a parallel sheet [34]. The observed $\Delta\nu$ values (217–234 cm^{-1}) are very close to those observed in alkali metal formates (235 cm^{-1}), which are considered as representing an ionic structure. Inasmuch as the two stretching modes of the carboxylate group are affected in the same way in the ionic and in the

Table 3
Characteristic structural parameters of pure and mixed bismuth and lanthanide formates and acetates

Ligand[a]	Metal	$\bar{\nu}$/cm^{-1}		$\Delta\bar{\nu}$/cm^{-1}[b]	d/pm[c]	$r_{M^{3+}}$/pm[d]	
		ν_{as}(COO)	ν_s(COO)			CN = 6	CN = 9
Fm	Bi	1550	1325	225	531.0	117	–
	La	1578	1359	219	540.1	117.2	135.6
	Pr	1575	1358	217	534.3	113	131.9
	Sm	1578	1361	217	525.5	109.8	127.2
	Bi–La (1:1)	1592	1358	234	529.2		
	Bi–Pr (3:1)	1592	1355	237	531.1		
	Bi–Pr (1:1)	1576	1356	220	533.6		
	Bi–Pr (1:3)	1574	1358	216	534.9		
	Bi–Sm (1:1)	1572	1353	219	531.7		
Ac	Bi	1544	1397	147			
	La	1533	1437	96			
	Bi–La (1:1)	1527	1407	120			

[a] Fm = HCO_2; Ac = CH_3CO_2.
[b] $\Delta\bar{\nu} = \bar{\nu}_{as}(COO) - \bar{\nu}_s(COO)$.
[c] Interreticular spacing associated with the first diffraction line.
[d] Shannon–Prewitt crystal radii for two coordination numbers (CN) [18].

bridged structure, the observation of the same $\Delta\nu$ value seems quite reasonable, although the IR bands concerned are both shifted.

The fact that the $\Delta\nu$ values obtained in the acetates are different can be ascribed to the presence of a distinct coordination mode, the acetate group being in a chelating position, which causes the $\Delta\nu$ value to decrease.

Within the pure $Ln(Fm)_3$ series (Ln is La, Pr, Sm), comparison between the d values and the ionic radii of Ln^{3+} indicates that the smaller the radius of the lanthanide ion, the smaller also the interreticular spacing, suggesting lattice contraction. Inside the Bi–Pr series, the d parameter increases with the praseodymium content.

3.4. X-ray diffraction studies of the thermal degradation products

The pure and mixed carboxylates synthesized in this work were systematically exposed to calcination in air. The formation of different solid phases was followed by X-ray diffractometry. Table 4 summarizes the results observed with the formate and acetate precursors. Except for the samples heated at 1123 or 1373 K, which are residues of TGA experiments, the compounds were heated in air for 16 h at the given temperature.

The formation of pure α-Bi_2O_3 was systematically confirmed after calcination of pure Bi(III) formate, triacetate, tripropionate, oxalate and lactate. The specific surface areas of these bismuth oxide samples, as measured according to the BET method, were, however, found to be closely dependent on the starting precursor. Values of 0.52 and

Table 4
XRD identification of the thermal decomposition products of pure and mixed Bi and Ln carboxylates

Compound	648 K	673 K	788 K	823 K	973 K	1123 K	1373 K
$Bi(HCO_2)_3$	α-Bi_2O_3 Bi_2CO_5			α-Bi_2O_3	α-Bi_2O_3		
$La(HCO_2)_3$					La_2O_3 [a]		
$Sm(HCO_2)_3$				Sm_2O_3 Sm_2CO_5	Sm_2O_3	Sm_2O_3	
$Pr(HCO_2)_3$				Pr_6O_{11}	Pr_6O_{11}	Pr_6O_{11}	
$La(CH_3CO_2)_3$						La_2O_3	
$Bi_{0.5}La_{0.5}(HCO_2)_3$		La_2CO_5 β-Bi_2O_3	La_2O_3 β-Bi_2O_3 La_2CO_5	La_2O_3 β-Bi_2O_3 La_2CO_5	β-Bi_2O_3 La_2O_3 [a] "Bi–La–O" phase [b]	α-Bi_2O_3 La_2O_3 [a]	
$Bi_{0.5}La_{0.5}(CH_3CO_2)_3$		α-Bi_2O_3 β-Bi_2O_3 La_2CO_5					
$Bi_{0.5}Sm_{0.5}(HCO_2)_3$		α-Bi_2O_3 β-Bi_2O_3 Sm_2O_3 Sm_2CO_5		α-Bi_2O_3 β-Bi_2O_3 Sm_2O_3 Sm_2CO_5	α-Bi_2O_3 δ-Bi_2O_3 Sm_2O_3 "Bi–Sm–O" phase [c]	α-Bi_2O_3 Sm_2O_3	
$Bi_{0.5}Pr_{0.5}(HCO_2)$		β-Bi_2O_3 Pr_2CO_5	β-Bi_2O_3 Pr_6O_{11}	β-Bi_2O_3 Pr_6O_{11} "Bi–Pr–O" phase [d]			β-Bi_2O_3 Pr_6O_{11} "Bi–Pr–O" phase [d]
$Bi_{0.25}Pr_{0.75}(HCO_2)_3$		β-Bi_2O_3 Pr_2CO_5	β-Bi_2O_3 Pr_6O_{11}	β-Bi_2O_3 Pr_6O_{11}		β-Bi_2O_3 Pr_6O_{11}	
$Bi_{0.75}Pr_{0.25}(HCO_2)_3$				β-Bi_2O_3 Pr_6O_{11} "Bi–Pr–O" phase [d]			

[a] Easily hydrolysed into $La(OH)_3$.
[b] Agreement with the $Bi_{0.82}La_{0.18}O_{1.5}$ phase.
[c] Agreement with the $Bi_{1.73}Sm_{0.27}O_3$ phase.
[d] Agreement with the $Bi_{1.35}Pr_{0.65}O_3$ phase.

1.58 $m^2 g^{-1}$ were respectively obtained from Bi(III) triacetate and Bi(III) tripropionate precursors calcined at 673 K for 20 h. For comparison, Bi_2O_3 prepared from thermal degradation of commercial bismuth citrate (Bi(Hcit)) under the same conditions exhibits a specific surface area of 0.78 $m^2 g^{-1}$.

As regards the formate and acetate compounds, Table 4 suggests the following comments:

(i) Mixed Bi–Ln–O phases are systematically observed when mixed Bi–Ln formates are heated at 823 K or above.

(ii) In agreement with the TGA results mentioned above, bismuth or lanthanide oxocarbonates are detected in the temperature range 548–823 K.

(iii) When praseodymium is present, the mixed valence oxide Pr_6O_{11} was systematically obtained.

(iv) Bismuth(III) oxide is obtained in different crystal phases; it is, however, well known that the α-phase is the only stable phase at low temperature (below 893 K) [50]; in all cases the presence of praseodymium seems to stabilize the tetragonal β-form, which is metastable; the presence of the cubic δ-form, which is reported as stable in the temperature range 1000–1100 K, is suggested, furthermore, in the Bi–Sm sample heated at 973 K.

3.5. *XRD characterization of the molybdate catalysts*

Table 5 summarizes the nature of the various solid phases whose presence was detected by X-ray diffraction studies of the Bi-, Ln-, or Bi–Ln-based molybdate catalysts after heating of the MoO_3-supported formate precursors at 823 or 973 K. Observations related to the use of pure lanthanide nitrates as precursors are listed for comparison. Some selected patterns are illustrated in Fig. 3. These results suggest the following remarks.

Ternary M–Mo–O molybdate phases are systematically detected (M is Bi, Ln). In the presence of Bi and/or Pr, these phases are always of the α-type, $M_2Mo_3O_{12}$. In the equimolar Bi–Pr system, a mixture of $Bi_2Mo_3O_{12}$ and $Pr_2Mo_3O_{12}$ is found; for the two other compositions, the bismuth *or* the praseodymium α-molybdate is detected depending on which metal is the most abundant. The crystal structure of the $Ln_2Mo_3O_{12}$ phases has been described in the literature [51, 52]; upon heating in the temperature range 1173–1273 K, these compounds undergo phase transitions leading to a tetragonal structure. In the temperature range which is relevant for this work (823–973 K), both the lanthanum and the praseodymium compounds exhibit a monoclinic structure, like α-$Bi_2Mo_3O_{12}$, whereas the corresponding samarium compound belongs to another structural type. The formation of $Pr_2Mo_3O_{12}$ from MoO_3 and Pr_6O_{11} was shown to start at about 773 K, after preliminary transformation of Pr_6O_{11} into Pr_2O_3 [52].

In the lanthanum case, the XRD patterns suggest the presence of another phase which seems not to be described in the literature, but shows interreticular spacing values which are close to those reported for samarium hexamolybdate, $Sm_2Mo_6O_{21}$. These data could therefore indicate the formation of $La_2Mo_6O_{21}$, although literature

Table 5
Phases detected by XRD in the various molybdate-type catalysts prepared from bismuth and lanthanide nitrates or carboxylates.

Sample no.	Precursor [a]	Catalysts calcined at 823 K	Catalysts calcined at 973 K
1	$La(NO_3)_3$	Mixed phase [b]	
2	$Pr(NO_3)_3$	$Pr_2Mo_3O_{12}$ [e]	
3	$Sm(NO_3)_3$	$Sm_2Mo_2O_9$ Other phase [c]	$Sm_2Mo_6O_{21}$ Other phase [c]
4	$Bi(HCO_2)_3$	$Bi_2Mo_3O_{12}$	
5	$La(HCO_2)_3$		Mixed phase [b]
6	$Pr(HCO_2)_3$	$Pr_2Mo_3O_{12}$ [e]	
7	$Sm(HCO_2)_3$		$Sm_2Mo_6O_{21}$ Other phase [c]
8	$Bi(HCO_2)_3 + Pr(HCO_2)_3$ (1/1)	$Bi_2Mo_3O_{12}$ $Pr_2Mo_3O_{12}$ [e]	
9	$Bi(HCO_2)_3 + La(HCO_2)_3$ (1/1)		$Bi_2Mo_3O_{12}$ Mixed phase [b,d,e]
10	$Bi_{0.5}La_{0.5}(HCO_2)_3$		$Bi_2Mo_3O_{12}$ [d,e]
11	$Bi_{0.75}Pr_{0.25}(HCO_2)_3$	$Bi_2Mo_3O_{12}$	
12	$Bi_{0.5}Pr_{0.5}(HCO_2)_3$	$Pr_2Mo_3O_{12}$ $Bi_2Mo_3O_{12}$ [e]	
13	$Bi_{0.25}Pr_{0.75}(HCO_2)_3$	$Pr_2Mo_3O_{12}$	

[a] The precursors noted as A + B (1/1) are mechanical mixtures of precursors A and B in equimolar ratio.
[b] La-containing phase akin to $Sm_2Mo_6O_{21}$ ($La_2Mo_6O_{21}$ suggested, see text).
[c] Unidentified phase.
[d] Hypothetical presence of Bi_2La alloy.
[e] Presence of small amounts of ε-MoO_3.

based on previous experiments does not mention this phase as a product of the solid state reaction between La_2O_3 and MoO_3, whereas the corresponding praseodymium and samarium compounds are obtained at about 990 K [53].

In both the Bi–Pr and Bi–La associations, comparative catalysts were prepared from mechanical mixtures of the pure bismuth and lanthanide formates, according to the same experimental procedure as described above. As indicated in Table 5, these catalysts are in no way different from those prepared from mixed coprecipitated precursors.

Thermal decomposition of MoO_3-supported samarium triformate at 973 K apparently results in the formation of samarium hexamolybdate, $Sm_2Mo_6O_{21}$. It should, however, be noted that the same phase is formed upon heating samarium(III) nitrate at the same temperature, while the β-molybdate $Sm_2Mo_2O_9$ is produced when $Sm(NO_3)_3$ is heated at 823 K. The decomposition temperature and not the precursor nature is thus clearly responsible for the occurrence of β-molybdate in these samples: conversion of the β-molybdate into the hexamolybdate occurs in the presence of excess MoO_3 according to the equation

$$Sm_2Mo_2O_9 + 4MoO_3 \rightarrow Sm_2Mo_6O_{21}$$

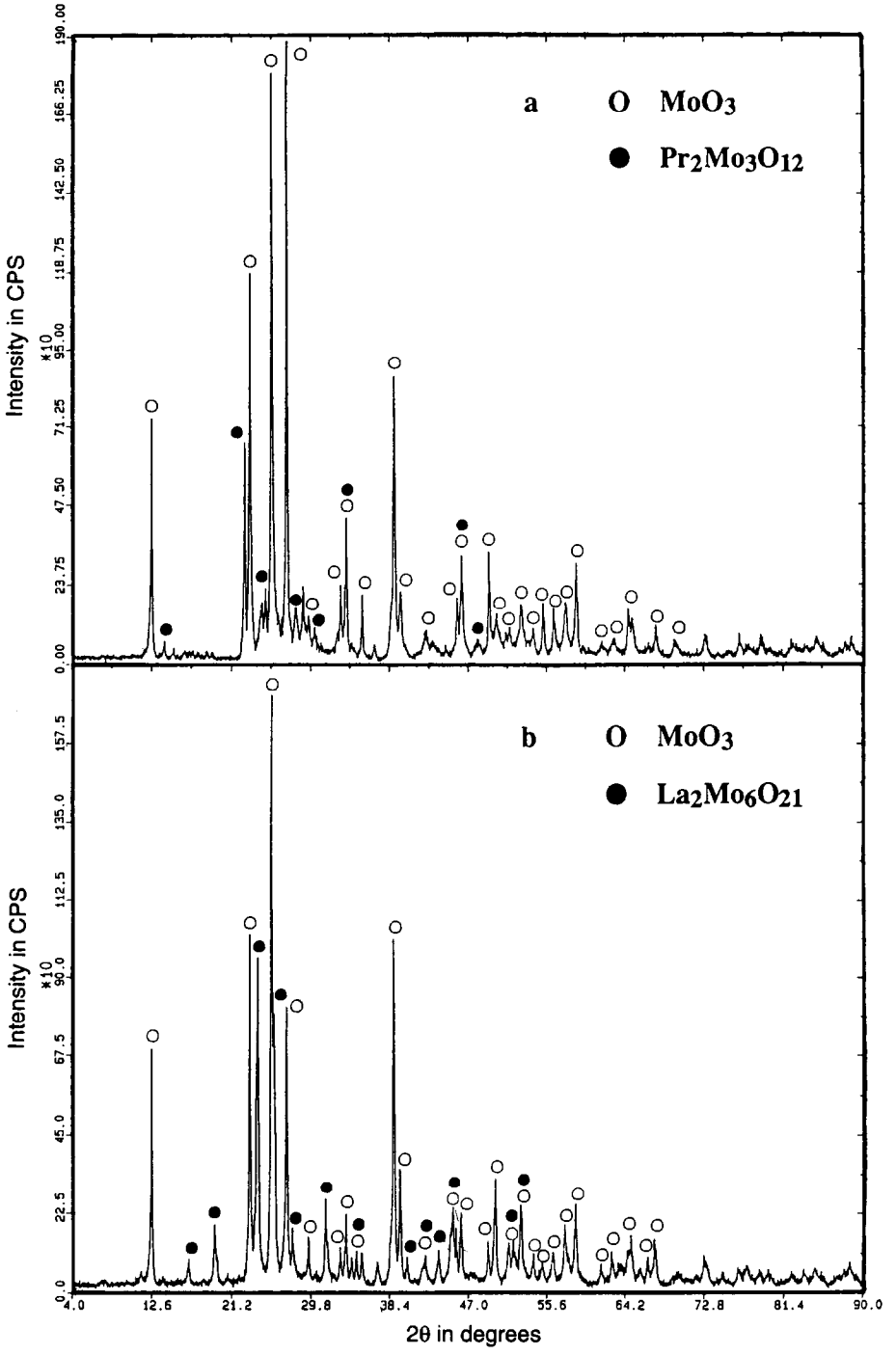

Fig. 3. X-ray diffraction spectrum of (a) MoO_3-supported praseodymium(III) triformate calcined at 823 K and (b) MoO_3-supported lanthanum(III) triformate calcined at 973 K.

Furthermore, in several cases the XRD spectra provided evidence for additional phases which remain unidentified on the basis of the present ASTM database. These are most probably quaternary phases of the type "Bi–Ln–Mo–O". Such phases have been described in the literature but correspond exclusively to solid solutions having the stoichiometry $Bi_{2-x}Ln_xMoO_6$ [54, 55], obtained by solid state reaction between the concerned γ-molybdates ($Bi_2MoO_6 + Ln_2MoO_6$) at high temperature, e.g. 1123 K in the case of neodymium. The widest homogeneity range of this solid solution is observed in the case of the Bi–La association, i.e. for metals which, in their trivalent ionic form, have exactly the same ionic radius. The presence of γ-type phases, M_2MoO_6, has, however, never been observed in our samples; equivalent phases of the α-type, displaying the stoichiometry $Bi_{2-x}Ln_xMo_3O_{12}$, whose presence is suggested by our results, seem not to be mentioned in the literature.

3.6. *IR investigations of the molybdate catalysts*

Selected samples in which new molybdate phases appeared were submitted to analysis by infrared spectroscopy. Attention was focussed on the 1000–400 cm^{-1} range in which the absorption bands related to the Mo–O and Ln–O–Mo vibrations are expected. They were compared with the results of IR investigations published in the literature. Typical IR spectra are shown in Figs. 4 and 5.

Reference IR spectra of the MoO_3 support were recorded after heating this oxide at the two temperatures selected for the calcination of the MoO_3-supported carboxylates,

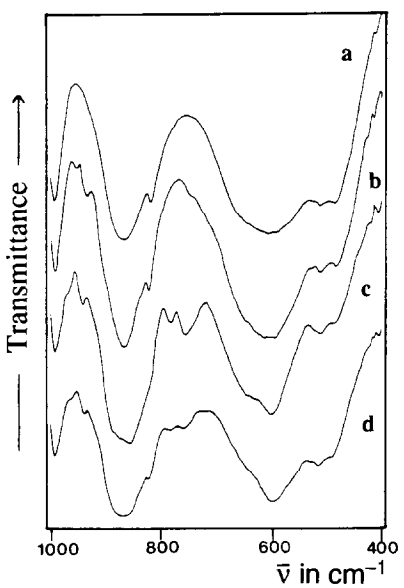

Fig. 4. Infrared spectra of (a) pure MoO_3 support, (b, c, d) MoO_3-supported molybdate catalysts calcined at 823 K. Precursors used are (b) Bi(III) formate, (c) Pr(III) formate, (d) (1:1) mechanical mixture of Bi(III) formate and Pr(III) formate.

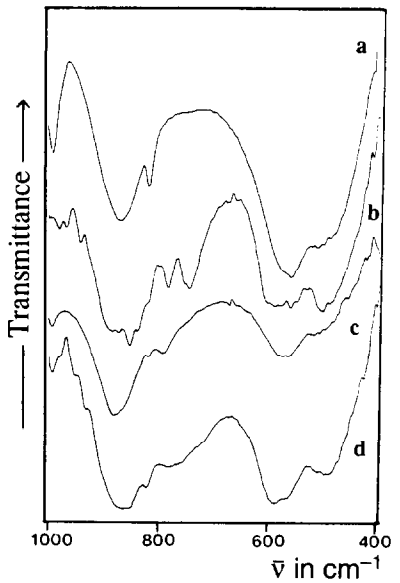

Fig. 5. Infrared spectra of (a) pure MoO_3 support and (b, c, d), MoO_3-supported molybdate catalysts calcined at 973 K. Precursors used are (b) Sm(III) formate, (c) La(III) formate, (d) mixed Bi–La (1:1) formate.

i.e. 823 and 973 K. After heating at 823 K (Fig. 4(a)), the IR spectrum is mainly characterized by a narrow line at 990 cm^{-1}, two broad bands at 867 and 607 cm^{-1}, and a rather well-defined shoulder at 820 cm^{-1}. Upon heating at 973 K (Fig. 5(a)), the shape of the IR spectrum remains quite similar but with narrowing of the two above-mentioned broad bands which improves the resolution of the 820 cm^{-1} band.

In the catalyst made from calcination of MoO_3-supported bismuth formate at 823 K (Fig. 4(b)), additional IR bands appear at 951 and 932 cm^{-1}. According to the literature [56–58], they correspond to the α-$Bi_2Mo_3O_{12}$ molybdate, in agreement with the XRD observations (see Table 5). In the related sample prepared from praseodymium formate at the same temperature (Fig. 4(c)), two spectral regions are more specifically altered when compared with the pure support. New IR bands undoubtedly appear at 940, 784 and 756 cm^{-1}, accompanied by a shoulder at 970 cm^{-1}. This shoulder, as well as the 940 cm^{-1} band, seems to be equivalent to the two additional bands mentioned in the preceding sample made from Bi formate. They probably correspond to vibrations of M–O–Mo bonds in α-type molybdate phases $M_2Mo_3O_{12}$ (M is Bi or Pr).

In the catalysts containing simultaneously Bi and Pr, the general shape is quite similar to the previous ones, apart from slight variations in two spectral regions: 975–900 and 800–725 cm^{-1}. The IR spectrum corresponding to the Bi–Pr (1/3) precursor is shown as an example in Fig. 4(d). When going from pure Pr to pure Bi through the various intermediate Pr:Bi compositions, the following features are noticed: in the 800–725 cm^{-1} region, peaks initially present at 784 and 756 cm^{-1} in the

Pr-rich samples gradually disappear as the bismuth content increases; in the 975–900 cm^{-1} region, IR bands characteristic of the pure M–Mo–O phases are shifted.

The IR spectrum of the catalyst made from MoO_3-supported samarium triformate calcined at 973 K is presented in Fig. 5(b), and clearly differs from the reference spectrum of pure MoO_3 heated at the same temperature (Fig. 5(a)), mainly through the presence of well-resolved bands at 969, 887, 856 and 785 cm^{-1}, undoubtedly demonstrating the presence of a new phase. Bands appearing at similar positions (965, 892 and 794 cm^{-1}) are also observed in the IR spectrum of a comparative catalyst prepared from samarium nitrate (impregnation from aqueous medium), inasmuch as the samples are calcined at the same temperature. According to the literature [53], bands at about 960, 880 and 790 cm^{-1} are characteristic of lanthanide hexamolybdates, and so these IR results reinforce the earlier interpretation based on X-ray diffraction measurements. It should furthermore be mentioned that the corresponding IR spectra obtained with the catalysts made from samarium nitrate after calcination at a lower temperature (823 K) exhibit a quite different shape, the above-mentioned characteristic bands being absent or much less intense, and replaced by others at 944, 788 and 753 cm^{-1}.

Infrared spectra of lanthanum-based molybdate catalysts are shown in Figs. 5(c) and 5(d). They correspond respectively to the systems in which pure lanthanum triformate and a mixed Bi–La (1:1) formate were used as precursors and calcined on MoO_3 at 973 K. When compared with the reference spectrum of pure MoO_3 heated at the same temperature (Fig. 5(a)), the main differences are due to the occurrence of new bands at 884 and 793 cm^{-1} which, according to the former comments on the samarium-based catalysts, could be interpreted as indicating the presence of lanthanum hexamolybdate on the surface. This is in agreement with the assumptions formulated in the framework of the XRD analysis. In the IR spectrum of the Bi–La molybdate catalyst (Fig. 5(d)), characteristic bands appear at 952, 775 and 586 cm^{-1}. The first was already noted as being compatible with α-$Bi_2Mo_3O_{12}$, which has been detected by XRD (see Table 5), the two others being similar to absorption bands present in the IR spectra of Sm- or Pr-based molybdate catalysts. The IR spectrum of an analogous catalyst made from an equimolar mixture of $BiFm_3$ and $LaFm_3$ under identical experimental conditions was found to be strictly equivalent to the previous one.

4. Conclusions

Short-chain carboxylate compounds of bismuth, lanthanum, samarium and praseodymium are shown to be of interest as precursors for the formation of specific molybdate-type phases upon thermal degradation in air on MoO_3 support. When bismuth and the rare earth element are incorporated simultaneously, experimental arguments from X-ray diffraction and infrared spectroscopy widely suggest the formation of mixed formato and acetato compounds displaying structures which are closely related to those of the pure compounds, in agreement with the similarity of the ionic radii of the concerned species. When mixed Bi–Ln systems are calcined at 973 K, the lanthanide nature is found to favour the formation of either α-type $M_2Mo_3O_{12}$ phases (Ln is La, Pr), or hexamolybdate phases, $M_2Mo_6O_{21}$ (Ln is Sm). Furthermore, this

work emphasizes the fact that careful FTIR investigations are invaluable in helping to elucidate the actual nature of supported phases in multicomponent or multiphasic molybdate-type catalysts. This is definitely an advantage for the characterization of supported phases which cannot be identified by X-ray diffraction, as would be the case either at low overall loading of the active phase on the support or when amorphous phases are generated.

Acknowledgements

The authors gratefully acknowledge financial support from the National Fund for Scientific Research (Brussels, Belgium) and from the "Institut pour l'Encouragement de la Recherche Scientifique dans l'Industrie et l'Agriculture" (I.R.S.I.A., Belgium) for the fellowship allotted to O.T. They are grateful to Prof. B. Delmon for access to the BET equipment and to Dr. J. Naud for his help in performing the X-ray diffraction experiments.

References

[1] A. Wold and K. Dwight, J. Solid State Chem., 88 (1990) 229.
[2] G.S. Sodhi and J. Kaur, Z. Naturforsch. Teil B, 47 (1992) 1297.
[3] M.G. Ambia, M.N. Islam and M. Obaidul Hakim, J. Mater. Sci., 28 (1993) 2659.
[4] H. Cui, R.D. Pike, R. Kershaw, K. Dwight and A. Wold, J. Solid State Chem., 101 (1992) 115.
[5] B.L. Druz', A.I. Dyadenko, Yu.N. Evtukhov, M.Ya. Rakhlin and V.E. Rodionov, Bull. Acad. Sci. USSR, Inorg. Mater., 26 (1989) 24 (Izv. Akad. Nauk SSSR, Neorg. Mater., 26 (1989) 34).
[6] D.S. Bem and H.-C. Zur Loye, J. Solid State Chem., 104 (1993) 467.
[7] H. Yoshimatsu, Y. Miura, A. Osaka, H. Kawasaki and S. Ohmori, J. Mater. Sci., 25 (1990) 5231.
[8] C.N.R. Rao (Ed.), Chemistry of Advanced Materials, Blackwell Scientific Publishers, Oxford, 1993.
[9] P. Courty, H. Ajot, C. Marcilly and B. Delmon, Powder Technol., 7 (1973) 21.
[10] C. Marcilly, P. Courty and B. Delmon, J. Am. Ceram. Soc., 53 (1970) 56.
[11] S.L. Furcone and Y.-M. Chiang, Appl. Phys. Lett., 52 (1988) 2180.
[12] N.H. Wang, C.M. Wang, H.-C.I. Kao, D.C. Ling, H.C. Ku and K.H. Lii, Jpn. J. Appl. Phys., 28 (1989) L1505.
[13] A. Aoki, Jpn. J. Appl. Phys., 29 (1990) L270.
[14] T. Asaka, Y. Okazawa, T. Hirayama and K. Tachikawa, Jpn. J. Appl. Phys., 29 (1990) L280.
[15] M.S.G. Baythoun and F.D.R. Sale, J. Mater. Sci., 17 (1982) 2757.
[16] C.-C. Chang and H.-S. Weng, Ind. Eng. Chem. Res., 31 (1992) 1615.
[17] M. Amala Sekar, G. Dhanaraj, H.L. Bhat and K.C. Patil, J. Mater. Sci.: Mater. in Electronics, 3 (1992) 237.
[18] R.D. Shannon, Acta Crystallogr. Sect. A, 32 (1976) 751.
[19] D. Gazzoli, A. Anichini, S. De Rossi, M. Inversi, M. Lo Jacono, P. Porta and M. Valigi, J. Catal., 119 (1989) 227.
[20] R.J.H. Voorhoeve, D.W. Johnson, Jr., J.P. Remeika and P.K. Gallagher, Science, 195 (1977) 827.
[21] T. Seiyama, Catal. Rev. Sci. Eng., 34 (1992) 281.
[22] Y. Takasu, S. Nishibe and Y. Matsuda, J. Catal., 49 (1977) 236.
[23] S. Sugiyama, Y. Matsumura and J.B. Moffat, J. Catal., 139 (1993) 338.
[24] J.M. Lopez Nieto, J.L.G. Fierro, L. Gonzalez Tejuca and G. Kremenic, J. Catal., 107 (1987) 325.
[25] G. Kremenic, J.M. Lopez Nieto, J.M.D. Tascon, L. Gonzalez Tejuca and S.W. Weller, Ind. Eng. Chem. Res., 26 (1987) 1419.

[26] G. Kremenic, J.M.L. Nieto, J.M.D. Tascon and L. Gonzalez Tejuca, J. Less-Common Metals, 138 (1988) 47.
[27] G. Kremenic, J.M.L. Nieto, J.L.G. Fierro and L. Gonzalez Tejuca, J. Less-Common Metals, 135 (1987) 95.
[28] V. Cortes Corberan and L. Gonzalez Tejuca, J. Coll. Interface Sci., 129 (1989) 270.
[29] J.M.D. Tascon, S. Mendioroz and L. Gonzalez Tejuca, Z. Phys. Chem. Neue Folge, 124 (1981) 109.
[30] S. Nakayama, M. Sakamoto, K. Matsuki, Y. Okimura, R. Ohsumi, Y. Nakayama and Y. Sadaoka, Chem. Lett., (1992) 2145.
[31] K. Nag and A. Roy, Thermochim. Acta, 17 (1976) 247.
[32] P. Sujatha Devi and M. Subba Rao, Thermochim. Acta, 15 (1989) 181.
[33] P. Sujatha Devi and M. Subba Rao, Mater. Lett., 16 (1993) 14.
[34] C.-I. Stahlanske, Acta Chem. Scand., 23 (1969) 1525.
[35] A.P. Pisarevskii, L.I. Martynenko and N.G. Dzyubenko, Russ. J. Inorg. Chem., 35 (1990) 843.
[36] O. Sorbye and I. Kruse, Acta Chem. Scand., 16 (1962) 1662.
[37] J.D. Donaldson, J.F. Knifton and S.D. Ross, Spectrochim. Acta, 20 (1964) 847.
[38] N.M. Chaplygina and L.S. Itkina, Russ. J. Inorg. Chem., 26 (1981) 1667.
[39] G.B. Deacon and R.J. Phillips, Coord. Chem. Rev., 33 (1980) 227.
[40] R. Bonnaire, C.R. Acad. Sci. Paris, Série B, 266 (1968) 1415.
[41] G. Gattow and H. Schwank, Z. Anorg. Allg. Chem., 382 (1971) 49.
[42] A.I. Grigorev, Russ. J. Inorg. Chem., 8 (1963) 409.
[43] W. Harrison and J. Trotter, J. Chem. Soc., Dalton Trans., (1972) 956.
[44] S.I. Troyanov and A.P. Pisarevskii, Koord. Khim., 17 (1991) 909.
[45] A. Telle, Arch. Pharm., 246 (1909) 484.
[46] J.R. Ferraro and M. Becker, J. Inorg. Nucl. Chem., 32 (1970) 1495.
[47] G.R. Rao, K.C. Patil and C.N.R. Rao, Inorg. Chim. Acta, 4 (1970) 215.
[48] K.C. Patil, G.V. Chandrashekhar, M.V. George and C.N.R. Rao, Can. J. Chem., 46 (1968) 257.
[49] D.G. Karraker, J. Inorg. Nucl. Chem., 31 (1969) 2815.
[50] J.W. Medernach and R.L. Snyder, J. Am. Ceram. Soc., 61 (1978) 494.
[51] K. Nassau, H.J. Levinstein and G.M. Loiacono, J. Phys. Chem. Solids, 26 (1965) 1805.
[52] L.A. Drobyshev, V.I. Ponomarev, I.T. Frolkina and N.V. Belov, Sov. Phys.—Cristallogr., 15 (1970) 391.
[53] L.Z. Gokhman, G.V. Lysanova, D.A. Dulin and D.V. Pashkova, Russ. J. Inorg. Chem., 19 (1974) 1106.
[54] E.G. Khaikina, L.M. Kovba, Z.G. Bazarova and M.V. Mokhosev, Russ. J. Inorg. Chem., 30 (1985) 1356.
[55] E.G. Khaikina, L.M. Kovba, Z.G. Bazarova, V.V. Khakhinov and M.V. Mokhosev, Russ. J. Inorg. Chem., 30 (1985) 1358.
[56] I. Matsuura, R. Schuit and K. Hirakawa, J. Catal., 63 (1980) 152.
[57] F. Trifiro, H. Hoser and R.D. Scarle, J. Catal., 25 (1972) 12.
[58] M. El Jamal, M. Forissier and G. Coudurier, React. Kinet. Catal. Lett., 37 (1988) 34.